**Proceedings of the ASME 2009 International Design Engineering Technical Conferences &
Computers and Information in Engineering Conference
IDETC/CIE 2009
August 30 - September 2, 2009, San Diego, California, USA**

DETC2009-86661

VOXEL-BASED INTERACTIVE HAPTIC SIMULATION OF DENTAL DRILLING

Jun Wu[a], Ge Yu[a], Dangxiao Wang[a], Yuru Zhang[a], and Charlie C. L. Wang[b]
[a] Beihang University, 100191, Beijing, China (e-mail: wujun@me.buaa.edu.cn)
[b] The Chinese University of Hong Kong, Shatin, N.T., Hong Kong, China (e-mail: cwang@mae.cuhk.edu.hk)

ABSTRACT

Haptics is one of the most important sensations for dentists to prepare cavity in dental surgery, which is however not easy to simulate in a computer system because of the large drilling force and the small speed of movement and material removal. In this paper, we present a fully voxel-based approach to interactively simulate dental drilling. Different from those voxel/mesh hybrid models, the drilling forces are computed directly from the voxel-representation while considering the factors of teeth's material properties, the posture and forward speed of dentist's drill and the contact surface area. To overcome force discontinuity caused by removal of tooth material, we define two layers of voxels on drill, where the boundary voxels are only employed to compute force feedback and the interior voxels are adopted to remove materials from teeth. The experimental result shows that our force model can produce smooth and large force feedback at a slow movement on haptic devices. Other than haptic rendering, a real-time filtering method directly using voxel representation has also been developed to improve visual rendering in dental simulation.

Keywords: *Haptic rendering, drilling force modeling, voxel model, dental simulation, visual rendering*.

1 INTRODUCTION

Cavity preparation is an important procedure in dental surgery. As illustrated in Fig.1, the dentist uses a high-speed rotating drill to remove the lesion part of the tooth to prepare a cavity which will then be filled with amalgam. During these operations, haptic sensation is very important for the dentist to operate successfully. However, how to train students on haptic sensation is a problem. Usually, students in dental training use plastic teeth or removed teeth from patients to practice these operations, but it is hard to simulate the stiffness of real teeth by plastic ones. Therefore, they cannot provide realistic force feedback to operators. Although the teeth removed from patients are stiff enough for dental training, it is difficult to find such a large quantity of removed teeth in practice. Therefore, there is a great demand for dental training system at the dentistry departments of medical schools.

Figure 1. Dental surgery training in medical schools.

Recently, many virtual reality dental training systems incorporating haptic feedback have been developed as alternatives to traditional training procedures (e.g., [1–3]). These systems provide realistic visual, sound and debris simulation, and the operations of students can be recorded for evaluation. However, as the magnitude of drilling force in dental surgery is relatively

large while the movement of drill is very small (in general around $0.5mm/s$ — see [4]), interactively simulating realistic force feedback is still a great challenge due to the limitation of drilling force model and the performance of haptic devices.

Most existing drilling force models (e.g., [2,5–7]) are based on the penetration depth or volume; however, our experiments show a different phenomenon that the magnitudes of drilling force is approximately linear to the forward moving velocity in dental drilling. Therefore, a new drilling force model is developed in this paper based on voxel-model. Unlike the mesh-based model used in our previous research on damping drilling force model [8], it is easier for the voxel representation to simulate material removal in reality. Our approach works well on voxels with different sizes, and realistic force feedback can be obtained using various drills such as fissure and round burs with different shapes.

Another feature of our method is that we exploit a simple and efficient visual rendering method. Different from other voxel based approaches, which use voxel model for force computation and mesh model for visual rendering, our method is fully voxel based. Point rendering, which avoids the complicated and time consuming mesh generation, is used to generate visual effect directly.

The rest of our paper is organized as follows. Section 2 analyzes the challenge of drilling simulation and reviews related works in voxel-based haptic rendering and drilling simulation. Section 3 details our method of haptic drill simulation. After briefing the visual rendering in section 4, section 5 shows the experimental data. Lastly, the paper ends with the conclusion section.

2 CHALLENGE OF DENTAL DRILLING SIMULATION

2.1 Criteria for dental drilling simulation

Compared with other bones of human body, teeth are small but with high stiffness. To provide a realistic simulation of drilling in dental cavity preparation, the features of tooth drilling are analyzed below. These features can actually serve as criteria to evaluate the performance of a dental drilling simulation.

Fidelity of force

There is a surface contact between the decayed tooth and the drill. The force felt by the dentist (named as the drilling force) is a combination of forces exerted on the whole contact area, which consists of resistance force to prevent the forward movement of drill and torque to prevent the rotation of drill. According to our experimental measurements [4], the resistance force in dental drilling is smooth and its magnitude is typically around $2N$. Moreover, the experiences of skillful dentists show that, the resistance force is dominant in the composition of drilling forces, and nearly no torque can be felt around the drilling axis. The reason why no torque can be felt is twofold: 1) the rotation speed is as high as up to $20,000rps$ which leads to little friction between the rotated drill and the tooth, and 2) the diameter of drill is about $0.8mm$ which is too small to generate significant torque. As a result, the torque around drilling axis is too subtle to be perceived.

Material removal

Some material will be removed as in consequence of the drilling force applied by the operator. It is a mechanical phenomenon involving the material's molecular structure. During the drilling process, the material removal velocity is equal to the forward velocity of the drill, typically smaller than $0.5mm/s$. The outcome of material removal is a cavity for medical treatment, which should cover the whole lesion part of the tooth. Therefore, different shapes of tooth decay result in different shape of cavity. Many types of cavities are introduced in [9]. A basic principle for cavity preparation is that the boundary of cavity should be smooth in order to reduce stress concentration.

Computational efficiency

Basically, there are three threads with different update rates in a haptic based dental drilling simulation: haptic rendering, material removal and visual rendering. The update of haptic rendering should be performed in $1kHZ$ [10], and the visual rendering must be at least $24HZ$. These all demand high computation performance. Furthermore, as the topology of the tooth is changed during drilling, the remaining material should be updated at an appropriate rate; otherwise, collision detection in the next simulation step will get wrong results.

Stability

During the simulation, there should have no obvious vibration. The stability of a haptic system generally refers to the maximum damping coefficient of damping force model and the maximum stiffness of spring force model which can be simulated stably. A realistic dental drilling simulation in general requests a high stability.

There are mainly three contradictions among these criteria.

1. *Fidelity and computational efficiency*. In order to achieve high computational efficiency, some simplifications of the drilling force model and material removal computation must be adopted, and these of course will weaken the fidelity of the system in return.
2. *Stability and high system-stiffness*. The ratio of the magnitude of drilling force over the movement of drill is very high in the dental simulation. However, the maximum damping coefficient that can be stably simulated is limited by the haptic device and haptic rendering. Generally, the design of rendering algorithm should exploit the optimized capability of selected haptic device while maintaining its stability.
3. *Stability and material removal*. When material is removed, discontinuity will be generated on the geometric model of drilled tooth. This may cause the discontinuity of force feed-

back and lead to unexpected vibration in the simulation.

The proposed method in this paper considers all the above contradictions and tries to provide a realistic simulation in both haptic and visual rendering.

2.2 Related works in drilling simulation

Compared with models in mesh representation, voxel-based models [11, 12] provide an intuitive representation to present solid formed by different tissues have different physical properties (e.g., stiffness) in different regions. Moreover, voxel representation is more suitable for material removal simulations such as virtual clay and virtual drilling, where removal can simply be implemented by deleting related voxels. Complex and time consuming mesh generation algorithm needs to be developed for such simulations in mesh representation (e.g., [6]).

There are several haptic enabled drilling systems based on voxel model developed in various biomedical applications, such as temporal bone surgery [5, 7], craniotomy [13], mastoidectomy [14], and dental surgery [2]. In these interactive simulations of material removal, different update rates are used for force feedback, visual feedback and/or material removal respectively. As physical based material removal is complicated in theory and has a great computational burden, geometry based approaches (e.g., the approaches based on penetration depth) are widely used to guarantee computational efficiency and stability. However, penetration depth will change frequently in material removal. Therefore, the traditional spring-damping force model will lead to force discontinuity if the force is computed directly from penetration depth. Such kinds of unwanted effect are serious in dental drilling as the displacement of drill in one haptic rendering cycle is relatively small.

In order to smooth the feedback force, Agus et al. [14] developed an analytical model of bone erosion as a function of applied drilling force and rotational velocity, and their model was verified with experimental data. McDonnell et al. [15] used the spring-based force based on the difference in the initial contact point on the surface and the current tool-tip position, where the force computation is independent of the current surface shape. Ruspini et al. proposed another method called *proxy blending* in [16], which smoothly interpolates the goal point from the old proxy point on the old surface to the new proxy point on the new surface. During the blending, the user cannot adjust the blending speed or the direction since the new surface should have been defined when the blending starts.

Although these methods can successfully prevent force discontinuity, none of them focused on the phenomenon that there is a nearly linear relationship between the drilling force and the forward velocity of the drill. Based on this experimental result, Liu et al. implemented a damping force model for dental drilling in [8], where the actual force in drilling on removed teeth was measured and compared with the force feedback in simulation.

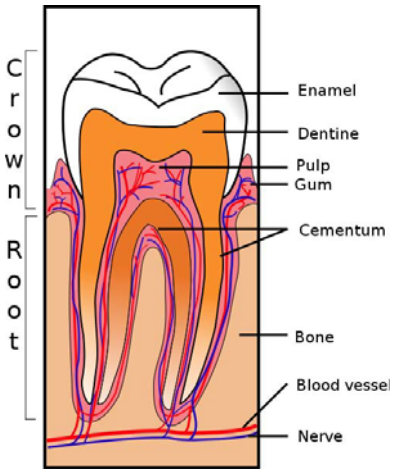

Figure 2. The illustration of tooth sections (captured from [17])

Although the magnitude of generated force is similar to the real surgery, the movement of virtual drill is inconsistent with the haptic device in their approach which affects the effectiveness of virtual training. Moreover, their tool is represented using only one point, which cannot simulate the variation in different drills. All these drawbacks are improved in this paper by using a voxel-based model and a novel material removal method.

As volume rendering is time consuming, Agus et al. [14] established a drilling system composed of two computers, where one computer is dedicated to volume rendering only. Other approaches (e.g., [2, 7]) avoided this by using mesh-based rendering method. The mesh model is reconstructed from voxel model for visual rendering. This impairs the simplicity and efficiency of voxel model, which provides intuitive information on the geometry and physical properties of teeth. We also developed a real-time filtering method, which is actually point-based rendering, for visual rendering of voxel model in dental drilling simulation. Our method can produce vivid visual results with acceptable computational cost.

3 VOXEL-BASED HAPTIC RENDERING

3.1 Tooth modeling

To simulate dental drilling realistically, tooth model in interactive simulation must have the information on both the detailed geometry and the interior physical properties at different regions. As voxel-model is used in our platform, both the geometry and the physical information can easily be represented by the flags of voxels.

At the geometry aspect, there are usually many tiny bumps and concavities on the surface of a tooth have a dimension of about $180 - 250\mu m$ [9]. In order to present these features accurately, the voxel size of an ideal tooth model should be at least

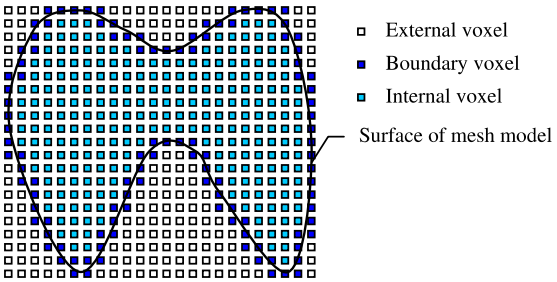

Figure 3. Voxels for a tooth are classified into external, internal and boundary ones.

smaller than these small features. The dimension of a tooth is around $5-8mm$. Therefore, the resolution of voxel model at $256 \times 256 \times 256$ is good enough.

A tooth is made up of different materials in a multi-layer structure (as shown in Fig. 2). The outer surface of a tooth is the enamel layer which is the hardest among the layers. Beneath the enamel is the dentin layer. It is a set of hard, porous, and yellow bone-like material surrounding the entire nerve. Dental pulp is soft tissue containing blood vessels and nerves. The carious lesion to be removed is a region of soft dark tissue that always exists on the surface of a tooth.

In our system, after obtaining the original data set of layered images from *computed tomography* (CT), we use the Mimics software from Materialise [18] for volume segmentation. The segmented slices are exported isotropic voxels with gray values indicating their physical properties. All the voxels in the *minimum axis aligned bounding box* (AABB) which contains the whole tooth are stored in an cubic array with the indices, (i, j, k), representing the location of a particular voxel and its position. Voxels in the cubic array are classified into external, internal and boundary voxels (see Fig.3). The physical properties are also stored together with the interior and boundary voxels to represent their drill damping coefficient, which will be used in the drilling simulation (as illustrated in Fig.4).

3.2 Modeling of drill

By letting the center of drill be the origin, the rotating axis be $z-$ direction and the axis of drill handle be $x-$ direction, we can model the drill in the same way as tooth does in voxel representation. As the shape and status of voxels of drill will never change during the simulation, to simplify the later material removal computation, we store the boundary and internal voxels of a drill in two separate voxel arrays. Also, the drill is sampled in the same size as the tooth model so that the material removal can be simulated at the same resolution. It is worth noting that sampling the drill at the same resolution is only valid for slow movement — i.e., the movement of drill in each material removal/update cycle is far smaller than the size of tooth voxel. Fortunately, it

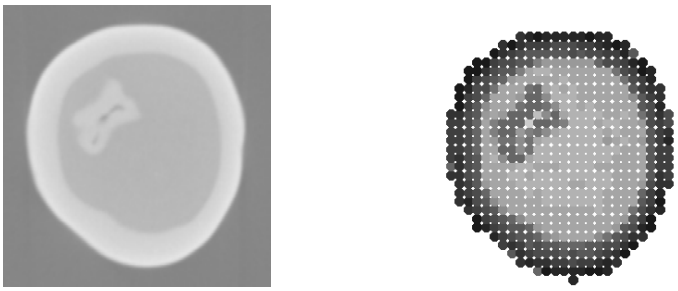

Figure 4. Physical properties are also stored at every voxel so that different sections can have different stiffness in drilling simulation. (a) CT slice sample. (b) An illustration of tooth sections with gray colors indicating gray values in CT slice.

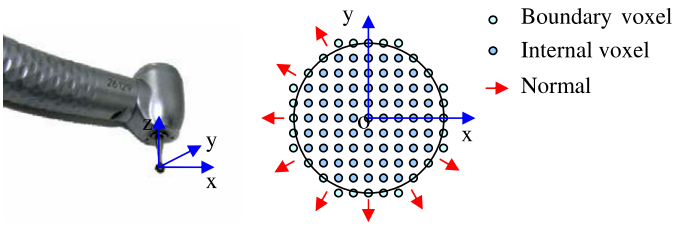

Figure 5. Modeling of a drill.

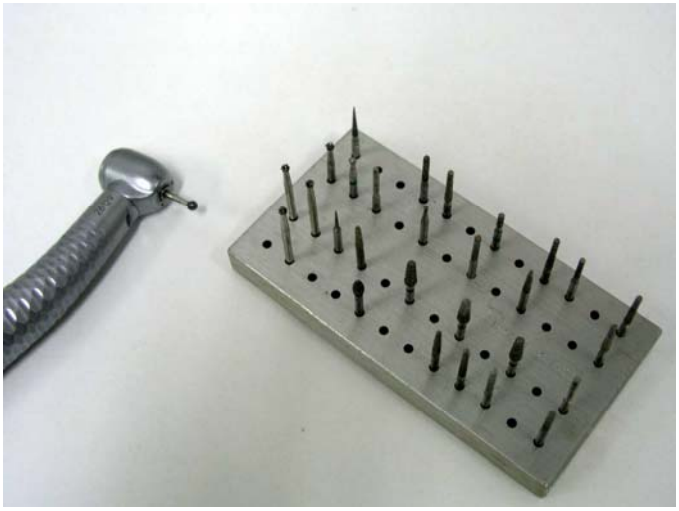

Figure 6. Different shapes of drills are employed in dental treatments.

is always the case in dental surgery simulations. Figure 5 shows the voxel model of a cylindrical drill, and Figure 6 gives various drills with different shapes.

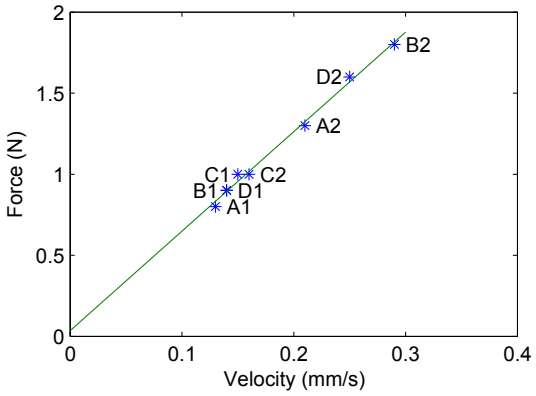

Figure 7. The experimental data of the tests given by four skillful dentists (each one performed twice) on real tooth — the resistance force and the drill moving velocity are approximately in a linear relationship.

3.3 Collision detection

Collision detection between the moving drill and the static tooth is conducted during the simulation to detect whether the drill has contacted the tooth and started to drill. It must also be reported by the collision detection algorithm which voxels are exactly overlapped. As only drill is moved, we detect all voxels of the drill to see if any of them is in the AABB box of the tooth. If this occurs, we then determine the corresponding voxels of the tooth for potential material update. Bounding volume hierarchies (BVH) can be employed to speed up the computation.

3.4 Force feedback calculation

In the dental drilling, the force between the drill and the tooth is mainly composed of two parts: 1) the force to resist the forward movement and 2) the torque to resist the rotation of the dental tool. As the torque in general is too small to be felt by dentists during the surgery, we focus on the simulation of resistance force below.

In order to find the relationship between the resistance force and the moving speed of drill in dental operation, we prepared a test bed to measure both the force and the speed of movement by sensors. Four skillful dentists were then invited to give dental drilling on a real tooth. Each of the dentists operated on two different parts of the tooth, and the average force and the average speed at each part are recorded. The experimental data are shown in Fig.7, where the maximum drill moving velocity (also the material removal velocity) is about $0.5mm/s$ and the corresponding feedback force is about $2N$. We can find from the test data that the relationship between the resistance force and the drill moving velocity is approximately linear.

From the above analysis, it is easy to find that the damping force model is very appropriate for the dental drilling simulation. The drill is in surface contact with the tooth during drilling, so

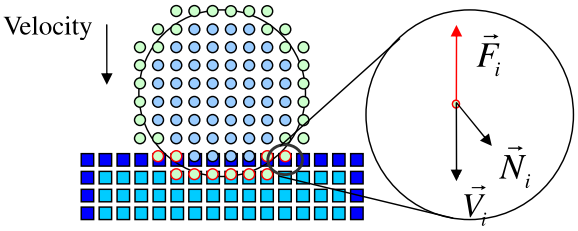

Figure 8. 2D illustration of resistance force calculation, where a cylindrical drill contacts the tooth. The force exerted on one voxel of the contact area is shown on the right, and the force felt by the dentist is a composition of all these forces.

we model the resistance force as

$$\vec{F} = f(\vec{V}, \mathbf{T}, A, B) \tag{1}$$

where $\vec{V}$ is the velocity of drill movement, $\mathbf{T}$ is the posture matrix of the drill, A is the area of contact, and B is the ratio of the resistance force to the drill moving velocity. The value of B can be obtained from the above tests (i.e., the slope of curve in Fig.7). As the ratio B is similar to the definition of damping, we name it as *drill damping* for the convenience of explanation below.

The force model is discretized on the voxel model so that it can be evaluated during the drilling simulation. For every boundary voxel of the drill, its position is used to check whether it has contacted the tooth. The corresponding resistance force at this voxel is then calculated according to the direction of its movement and the drilling tool's normal at this point (see Fig.8 for the illustration). The sum of resistance forces at all boundary voxels of the drill will be sent to the haptic device to simulate the resistance force felt by dentists, which is expressed as

$$\vec{F} = -\sum_{i=1}^{n} \vec{F}_i = -\sum_{i=1}^{n} b\cos(\vec{N}_i, \vec{V})\vec{V} \tag{2}$$

where n is the number of boundary voxels of drill that intersected with the tooth, b is ratio of drilling force to drill moving velocity, $\vec{N}_i$ is the normal vector of the $i-$th voxel, and $\vec{V}$ is the translational velocity.

In real dental surgery, when drilling on different layers of material with different drills, the ratio of resistance force to material removal velocity is different. We may determine the value of b in Eq.(2) by using the measured drilling force data. Suppose the drill damping of the tooth under cutting is B and there is no rotation in the drilling process. Then, we get

$$b = \frac{B}{\sum_{i=1}^{n} H(\cos(\vec{N}_i, \vec{V}))\cos(\vec{N}_i, \vec{V})} \tag{3}$$

with the *Heaviside step function* $H(\cdots)$.

3.5 Modeling of material removal

Our method for the material removal is geometry based. Geometrically, two solid bodies such as the tooth and the drill will never occupy a same space in $\Re^3$. Therefore, in the simulation, when the drill contacts the treated tooth, the corresponding voxels in the tooth should be removed.

The maximally allowed displacement $s_{\max}$ of drill is determined by the maximum velocity of the drill $v_{\max}$ as

$$s_{\max} = v_{\max}\Delta t \tag{4}$$

with Δt as the time step. In typical dental drilling, the maximum velocity $v_{\max}$ is about $0.5mm/s$, and Δt is $1ms$ which is governed by the haptic perception, then we have $s_{max} = 0.0005mm$. Suppose that at a time current t_i, the drill has contacted the tooth, the overlapped voxels are then removed immediately. In the next haptic cycle, the drill's movement is less than the maximally allowed displacement $s_{\max}$ of the drill. As $s_{max} = 0.0005mm$ is far below the voxel size of the tooth, this means that at the next time current t_{i+1} the drill will lose contact with the tooth. If so, the computed resistance force will be zero as our drilling force model is based on the contact area as well. When processing material removal in this way, the discontinuity of computed resistance force will occur frequently and will then make the haptic system unstable. This effect can be eliminated by using very high voxel resolution, which however will greatly increase the cost of computational time and memory and is impractical.

To overcome the discontinuity caused by the loss of contact, we proposed a two layer model based material removal method. That is, the voxels of a tooth is removed only when the interior voxels of the drill has overlapped with these tooth voxels. The boundary voxel layer of a drill is adopted for contact determination and resistance force calculation, while the interior voxels are used for material removal. After removing the corresponding tooth voxels, the tooth voxels overlapped by the boundary drill voxels will become the new surface of the tooth. Using this method, no matter what size the voxel is, the contact area is constant when removing material (i.e., voxels) from the tooth model. Thus, there is no force discontinuity. Figure 9 shows an illustration of our material removal method.

In practice, as the drilling velocity is relatively low, there is no need for surface updating at every haptic loop. The time span for the interior voxels to contact new surface is about $T = D_{voxel}/v_{max}$ with D_{voxel} being the voxel size and v_{max} being the maximum drilling velocity. Therefore, the optimal update rate of material removal is

$$f = 1/T = v_{max}/D_{voxel}. \tag{5}$$

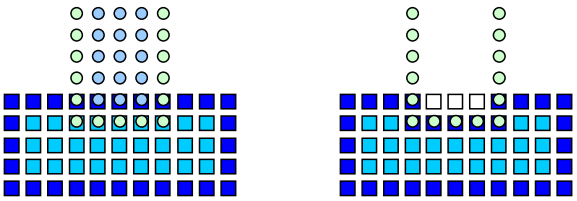

a) Before voxel removed b) After voxel removed

Figure 9. Material removal: (a) the status at the time current $t = t_i$ and (b) the status at $t = t_{i+1}$ where three voxels in the tooth have been removed. However, the contact area is constant during the material removal. For better illustration, internal voxels of the drill are not displayed in (b).

4 REAL-TIME VISUAL RENDERING

As the tooth model is represented by voxels, it is convenient to adapt point rendering directly using boundary voxels. Point rendering is a new technology developed in recent years for a variety of applications in computer graphics (ref. [19]). The steps in point rendering include the calculation of point normals and the normal filtering (see [20, 21]).

Different from the normal calculation of point cloud, which needs to construct a covariance matrix and determine its eigenvectors, our method is easier to compute as it employs the isotropic property of voxel models. The normal of a boundary voxel is computed by its 26 neighboring voxels; more specifically, for the corresponding sample point $\vec{p}_i$ of a boundary voxel, its normal is defined as

$$\vec{n}_i = \sum_{j \in N(i)} (\vec{p}_i - \vec{p}_j) \in \Re^3, \tag{6}$$

where $N(i) = \{j : \left\|\vec{p}_j - \vec{p}_i\right\| \leq \sqrt{3}d \cap \vec{p}_j \in tooth\}$ is the set of valid samples around $\vec{p}_i$, and d is the uniform distance between the isotropic voxels. The unit normal vector $\hat{n}_i$ of the sample point is obtained after the normalization of $\vec{n}_i$.

The displayed surface of the tooth model after the above normal computation is not smooth. We then exploit the bilateral filtering to process the normal vectors. The original bilateral filter is a nonlinear, feature preserving image filter. In our application, for a sample point p_i with the unit surface normal $\hat{n}_i$, the filtered normal at this sample is defined as

$$\hat{n}_i = \frac{\sum_{j \in N'(i)} W_c(\left\|\vec{p}_j - \vec{p}_i\right\|) W_s(d_{ij}) \hat{n}_j}{\sum_{j \in N'(i)} W_c(\left\|\vec{p}_j - \vec{p}_i\right\|) W_s(d_{ij})} \tag{7}$$

where W_c and W_s are standard Gaussian functions in the spatial domain and intensity domain respectively, $N'(i) = \{j :$

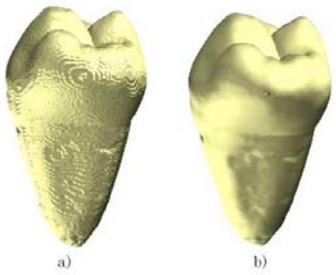

Figure 10. Bilateral filtering of normal: a) the visual effect using initial normals and b) the result of filtered normal.

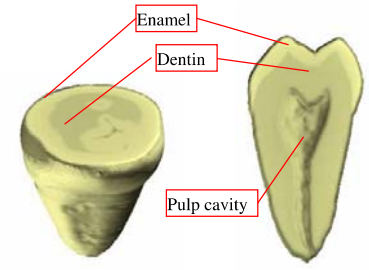

Figure 11. Different layers in tooth section view: different layers are shown in different colors according to their gray-values in raw data of CT slices.

$\left\|\vec{p}_j - \vec{p}_i\right\| \leq \sqrt{3}a \cap \vec{p}_j \in surface\ \ of\ \ tooth\}$, and d_{ij} is the "intensity difference" between two point normals $\hat{n}_i$ and $\hat{n}_j$. The intensity difference is defined to be the projection of the normal difference vector $(\hat{n}_i - \hat{n}_j)$ on the point normal $\hat{n}_i$, i.e.,

$$d_{ij} = \hat{n}_i \cdot (\hat{n}_i - \hat{n}_j). \tag{8}$$

Figure 10 shows an example of such normal filtering. This method can also be used to show different layers as illustrated in Fig. 11 if the *surface of tooth* in Eq.(7) is replaced by the *interface* of different sections.

During the drilling process, after some material has been removed from the original voxel model, we use the opposite direction of the drill's normal to represent the normal at sample voxels of the new surface.

5 EXPERIMENTAL RESULTS AND DISCUSSION

The proposed methods are implemented in VC++ 6.0 with GHOST SDK and OpenGL, and integrated into a dental drilling simulation system. This dental training system is composed of a haptic device and a half-silvered mirror to achieve collocated display between the visual and haptic sensation (see Fig.12). Previously developed simulation includes tooth surface probing, tooth

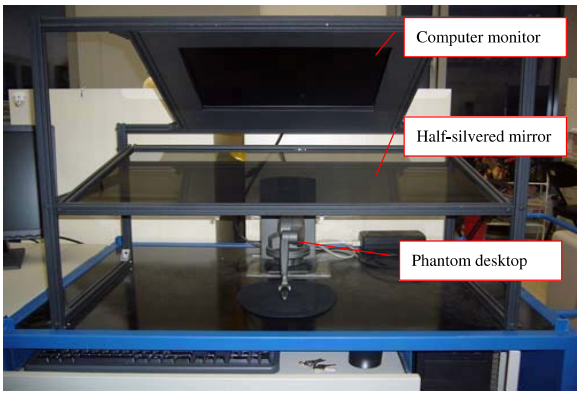

Figure 12. Our dental training system.

section probing, etc. This system is aimed at providing vivid dental training simulation in a Chinese dental school. The haptic device used in the system is the Phantom desktop from Sensable Technologies, and our computation is conducted on a PC with Intel Core2 Duo CPU, 2GB RAM, and an ATI Radeon X1550 display card with 256MB RAM.

The parameters for our initial test are as follows.

1. *Tooth*
   A volume of tooth $(10mm * 10mm * 10mm)$ is voxelized with voxel size of $0.1mm$. The drill damping coefficient of enamel layer is set as $4Ns/mm$, and dentin layer is $1Ns/mm$.
2. *Drill*
   A spherical drill (with diameter $d = 0.8mm$) and a cylinder drill (with diameter $d = 0.8mm$ and length $l = 1.0mm$) are also voxelized with the same voxel size as that of the tooth.
3. *Operation*
   The movement of the drill is perpendicular to the surface of the tooth with a velocity of around $0.5mm/s$. The velocity of operation is obtained by Phantom GHOST SDK. However, the direct velocity derived from position information is quite noisy, we thus use a threshold filter to smooth it. If the magnitude of velocity change between two consequent time step is larger than a threshold $\Delta = 0.1mm/s$, we set

$$\vec{V}_{t+1} = \vec{V}_t + \Delta * \frac{\vec{V}_{t+1} - \vec{V}_t}{\left\|\vec{V}_{t+1} - \vec{V}_t\right\|}. \tag{9}$$

4. *Update rates*
   We use the update rate at 1kHz for haptic rendering, and 30Hz for visual rendering. According to Eq. 5, the optimal update rate for material removal is $f = 5Hz$. As in the experiment, the operator's velocity is sometime bigger than the request of $0.5mm/s$. In practice, we choose 10Hz for all our tests.

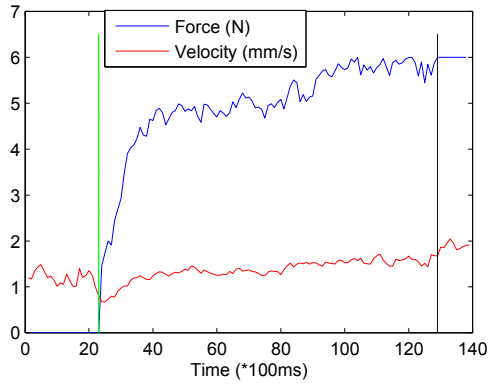

Figure 13. Drilling force and velocity relationship using a cylinder shape drill. On the left of the green line, the drill is in free space (does't contact the tooth); between the green line and black line, the drill is drilling on the tooth; on the right of the black line, the calculated drill force is larger than the maximum feedback force of Phantom, so we lower it down to $6N$.

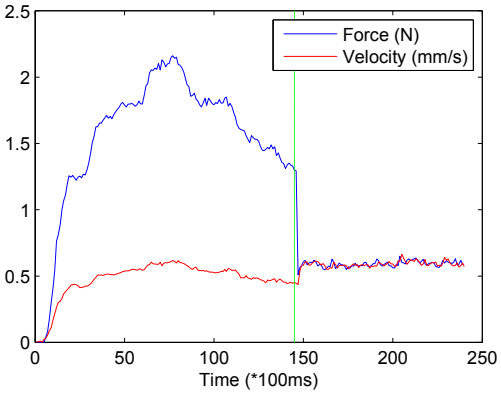

Figure 14. Force feedback of drilling on different sections of a tooth, where on the left of the green dot line is the drilling conducted on the enamel layer with velocity $0.5mm/s$ and then drilling on the dentin section is shown on the right.

We first test our system using a cylinder shape drill. The computed drilling force and its corresponding drill moving velocity are plotted in Fig.13. In Fig.14, we performed drilling on different sections of the tooth with a spherical drill. Fig. 15 shows two typical cavities prepared using a spherical drill.

We also evaluated our method on voxels with a larger size. A $10mm * 10mm * 10mm$ volume with voxel size $0.4mm$ and the same voxel size for a spherical drill are tested. Although it is not good for visual rendering at this resolution, we can still get stable feedback force as plotted in Fig 16.

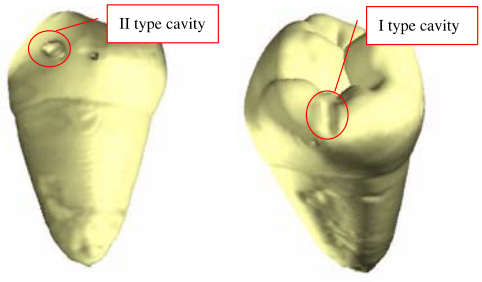

Figure 15. Two typical types of cavities prepared using our system by skillful dentists.

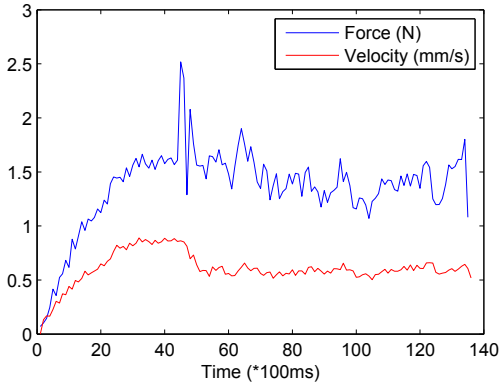

Figure 16. Drilling with large voxel, where the voxel size is chosen as $0.4mm$ for both the tooth and the drill models, the drill damping coefficient is $2.5Ns/mm$, and the drilling velocity is at around $0.5mm/s$

5.1 Discussion

The magnitude of feedback force in Fig. 14 and Fig. 16 is between $1.5 \sim 2.5N$, which is similar to the measured forces in our experimental drilling on real teeth. The measurements in real drilling versus our simulation are shown in Fig. 17, where the measured material removal velocity is maximally $0.5mm/s$.

There are no data on force and corresponding material removal velocity reported in other research papers of dental drill simulation. Therefore, we can only compare the result by this proposed method with our previous work on mesh-based tooth model [8]. The current system using Phantom desktop can generate up to $4Ns/mm$ damping coefficient, which is similar to the result that can be provided on the Omega system [8]. The Omega system has a better position resolution and can provide greater stiffness than Phantom. The current system can provide better cavity shape and more types of drills than [8].

During our test on different parameters, when trying to increase the damping coefficient, the Phantom system becomes unstable. We believe that it is caused by the noisy velocity derived from position. As the moving velocity of haptic device in our application is very low, the estimated error of velocity be-

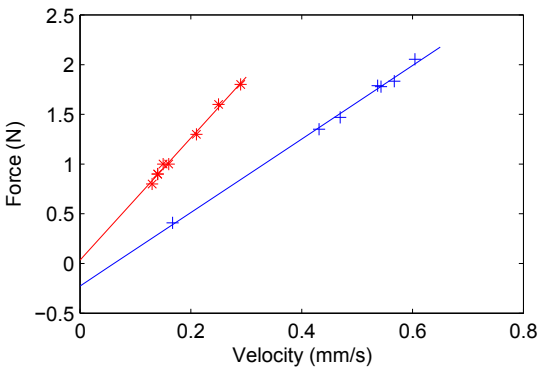

Figure 17. The relationship between feedback force and drilling velocity in real dental drilling (the red one) versus our simulation (the blue one). The simulation data are the same as that plotted in the left of Fig. 14.

comes larger, thus it leads to errors in force calculation. In dental drilling, the moving velocity is small and smooth. The change of velocity at two successive time steps should be small. Therefore, we use a threshold to smooth the velocity (see Eq. 9). The velocity will not get smoothed if the threshold is too big, whereas small threshold will decrease the credibility of the velocity which will lead to delay in force (when the operator stops drilling, he can still feel feedback force as it needs several time steps for the computing velocity to decrease to zero). In our experiment, the threshold is chosen empirically, which needs to be verified in the future. Haptic device with a more precise encoder or a velocity sensor can be employed to improve the performance.

While the computed drilling force feels similar to that in real dental drilling, the participated skillful dentists suggest that a supporting platform for the hand is greatly needed (see Fig. 1, the mandible of the patient acts as a supporting platform for dentist's hand), as without the platform, it is hard to perform a stable and precise drilling slowly (below $0.5mm/s$).

6 CONCLUSION

We present a dental drilling system based on voxel model in this paper. The feedback force is calculated using damping force model according to our initial drilling experiments on real teeth, which is less affected by the voxel size. A novel two layer based drilling update method is exploited to avoid force discontinuity on voxel models. We achieve continuous feedback force at around $2N$ with a low velocity ($0.5mm/s$) on different voxel sizes. Two kinds of drills are applied in the experiment to create cavities in different shapes. The simulation is realistic in force feedback and material removal.

In the future, more experiments will be conducted to further study the physical properties of tooth, and we are also planning to study the mechanical law behind material removal in drilling and to explore physical based simulation. Furthermore, the acceleration method of using parallel computing on GPU will be explored.

ACKNOWLEDGMENT

This work is supported by the National Science Foundation of China under grant *No*.60605027 and *No*.50575011, the National Hi-tech Research and Development Program of China under grant *No*.2007*AA*01*Z*310, the Hong Kong RGC/CERG grant CUHK/417508, and the open project "Research of GPU-Accelerated Force Rendering on Volumetric Model" of State Key Lab of Virtual Reality Technology and Systems of China. The authors would also like to thank Dr. Akiko Kato of Aichi-Gakuin University for sharing the CT data of teeth, and Materialise for providing the evaluation license of Mimics software.

REFERENCES

[1] Chen, L.-Y., Fujimoto, H., Miwa, K., Abe, T., Sumi, A., and Ito, Y., 2003. "A dental training system using virtual reality". In Computational Intelligence in Robotics and Automation, 2003 IEEE International Symposium on, pp. 430–434.

[2] Kim, L., and Park, S. H., 2006. "Haptic interaction and volume modeling techniques for realistic dental simulation". *The Visual Computer,* **22**(2), pp. 90–98.

[3] Marras, I., Papaleontiou, L., Nikolaidis, N., Lyroudia, K., and Pitas, I., 2006. "Virtual dental patient: a system for virtual teeth drilling". In Multimedia and Expo, 2006 IEEE International Conference on, pp. 665–668.

[4] Liu, G., Zhang, Y., and Townsend, W. T., 2008. "Force modelling for tooth preparation in dental training system". *Virtual Reality,* **12**(3), pp. 125–136.

[5] Petersik, A., Pflesser, B., Tiede, U., Hoehne, K. H., and Leuwer, R., 2002. "Haptic volume interaction with anatomic models at sub-voxel resolution". In HAPTICS '02: Proceedings of the 10th Symposium on Haptic Interfaces for Virtual Environment and Teleoperator Systems, p. 66.

[6] Wang, D., Zhang, Y., Wang, Y., Lee, Y.-S., Lu, P., and Wang, Y., 2005. "Cutting on triangle mesh: Local model-based haptic display for dental preparation surgery simulation". *IEEE Transactions on Visualization and Computer Graphics,* **11**(6), pp. 671–683.

[7] Morris, D., Sewell, C., Barbagli, F., Salisbury, K., Blevins, N. H., and Girod, S., 2006. "Visuohaptic simulation of bone surgery for training and evaluation". *IEEE Comput. Graph. Appl.,* **26**(6), pp. 48–57.

[8] Liu, G., Zhang, Y., Wang, D., and Townsend, W. T., 2008. "Stable haptic interaction using a damping model to im-

plement a realistic tooth-cutting simulation for dental training". *Virtual Reality,* **12**(2), pp. 99–106.

[9] Fan, M., and Zhou, X., 2000. *Operative Dentistry and Endodontics (In Chinese)*, second ed. People's Medical Publishing House.

[10] Salisbury, K., Conti, F., and Barbagli, F., 2004. "Haptic rendering: introductory concepts". *Computer Graphics and Applications, IEEE,* **24**(2), March-April, pp. 24–32.

[11] Avila, R. S., and Sobierajski, L. M., 1996. "A haptic interaction method for volume visualization". In VIS '96: Proceedings of the 7th conference on Visualization '96, pp. 197–204.

[12] McNeely, W. A., Puterbaugh, K. D., and Troy, J. J., 1999. "Six degree-of-freedom haptic rendering using voxel sampling". In SIGGRAPH '99: Proceedings of the 26th annual conference on Computer graphics and interactive techniques, pp. 401–408.

[13] Acosta, E., and Liu, A., 2007. "Real-time volumetric haptic and visual burrhole simulation". In Virtual Reality Conference, 2007. VR '07. IEEE, pp. 247–250.

[14] Agus, M., Giachetti, A., Gobbetti, E., Zanetti, G., and Zorcolo, A., 2003. "Real-time haptic and visual simulation of bone dissection". *Presence: Teleoper. Virtual Environ.,* **12**(1), pp. 110–122.

[15] McDonnell, K., Qin, H., and Wlodarczyk, R., 2001. "Virtual clay: a real-time sculpting system with haptic toolkits". In ACM Symposium on Interactive 3D Techniques, pp. 179–190.

[16] Ruspini, D., and Khatib, O., 1998. "Dynamic models for haptic rendering systems.". In Advances in Robot Kinematics Proceedings, pp. 523–532.

[17] "http://commons.wikimedia.org/wiki/tooth".

[18] Materialise. "Mimics". *www.materialise.com/mimics*.

[19] Kobbelt, L., and Botsch, M., 2004. "A survey of point-based techniques in computer graphics". *Computers and Graphics,* **28**(6), pp. 801–814.

[20] Lee, K.-W., and Wang, W.-P., 2005. "Feature-preserving mesh denoising via bilateral normal filtering". In CAD-CG '05: Proceedings of the Ninth International Conference on Computer Aided Design and Computer Graphics, IEEE Computer Society, pp. 275–280.

[21] Jones, T. R., Durand, F., and Desbrun, M., 2003. "Non-iterative, feature-preserving mesh smoothing". In ACM SIGGRAPH 2003, ACM, pp. 943–949.